for reductant attack, thus blocking a $k_0$ path similar to that observed here for tetrazole complexes. Additionally, the p$K_a$'s of these complexes are considerably higher (10 for the imidazole complex[32]) than those of our tetrazole complexes, thus suppressing the $k_1$ path at low pH where the chromium(II) reductions were followed, i.e., 0.10 M $HClO_4$ for the imidazole system[1c] and 1.2 M $HClO_4$ for the pyrazole system.[6b] The present study, however, points to the efficient operation of a tetrazole ring as an electron-transfer mediator, and, perhaps, if higher pHs are employed with the imidazole and pyrazole systems, evidence for inner-sphere electron transfer will become apparent in those systems as well.

**Acknowledgment.** R.J.B. thanks the Natural Sciences and Engineering Research Council of Canada for support of this work and D. Frick for some of the kinetic measurements. M.L.L. thanks J. Q. Searcy and R. G. Jungst for providing proton, $^{13}C$, and $^{15}N$ NMR data obtained by Lois Gerchman and L. Carey at SRI International.

**Registry No.** $[Co(NH_3)_5CN_4CN](BF_4)_2$, 87371-39-9; *N*-2-$[Co(NH_3)_5CN_4CH_3](BF_4)_2$, 87371-40-2; *N*-1-$[Co(NH_3)_5CN_4CH_3](ClO_4)_2$, 84927-29-7; $[Co(NH_3)_5CN_4CONH_2](BF_4)_2$, 87371-41-3; $[Co(NH_3)_5CN_4H](BF_4)_2$, 87371-43-5; hexaaquachromium(II), 20574-26-9; aquapentaamminecobalt(III) perchlorate, 13820-81-0.

**Supplementary Material Available:** A table of kinetic data (3 pages). Ordering information is given on any current masthead page.

(32) Harrowfield, J. M.; Norris, V.; Sargeson, A. M. *J. Am. Chem. Soc.* **1976**, *98*, 7282.

Contribution from the Pharmaceutical Institute, Tohoku University, Aobayama, Sendai 980, Japan, and Department of Chemistry, The Ohio State University, Columbus, Ohio 43210

# Magnetic Circular Dichroism Studies on [5,10,15,20-Tetrakis(1-methylpyridinium-4-yl)porphinato]iron and Some of Its Derivatives

NAGAO KOBAYASHI,*† MASAMI KOSHIYAMA,† TETSUO OSA,† and THEODORE KUWANA‡

*Received March 8, 1983*

Magnetic circular dichroism (MCD) spectra are reported for [5,10,15,20-tetrakis(1-methylpyridinium-4-yl)porphinato]iron(III) and -iron(II), $Fe^{III}$TMP and $Fe^{II}$TMP, and some of their derivatives in the near-UV to near-IR regions. Two proton equilibria existed between the three $Fe^{III}$TMP monomers with p$K_a$ values of ca. 5.7 and 12.3 while, after electrochemical reduction, an equilibrium was observed between the two $Fe^{II}$TMP monomers with a p$K_a$ of ca. 11.2. The species were in high-spin states except $Fe^{III}$TMP at pH >13 and $Fe^{II}$TMP at pH >12 (low spin). Porphyrin electronic structures of the coordination spheres on these species and their bis(imidazole) and bis(cyanide) derivatives are discussed in comparison with information on iron porphyrins and hemes previously studied.

## Introduction

Since its introduction in 1970,[1] 5,10,15,20-tetrakis(1-methylpyridinium-4-yl)porphine, TMP, and its metal complexes have been of particular interest among porphyrin researchers because of its stability and high solubility in water over a wide range of pH. In addition to several spectroscopic studies,[2-8] recent studies[9-13] have demonstrated in particular that the iron complex of this porphyrin, FeTMP, is an eminent catalyst for the electroreduction of oxygen. Irrespective of such an attractiveness, however, its mechanisms are not completely elucidated owing to simultaneous acid-dissociation and dimerization equilibria depending on pH and/or concentration.

Recently two papers[7,8] appeared on the electrochemical and spectral speciation of this porphyrin in water, in which emphasis was placed on acid-dissociation and monomer-dimer equilibria. In this study, therefore, we present the results of MCD on $Fe^{III/II}$TMP species in water. MCD spectroscopy has proven to be a powerful technique to verify the oxidation, spin and ligand states of chromophores.[14,15] Accordingly, by the use of MCD spectroscopy, it is expected that not only the information on proton equilibria is obtainable but also the porphyrin electronic structures of the coordination spheres can be discussed in comparison with information on iron porphyrins and hemes previously studied.

## Experimental Section

**(i) Materials.** Chemicals were commercially available guaranteed reagents and were used without further purification. $Fe^{III}$TMP(Cl) was prepared by the method of Fleischer.[1] The ratio of C:N:Fe was experimentally determined to be 44:7.9:0.98 as compared to theoretical values of 44:8:1. To generate $Fe^{II}$TMP from $Fe^{III}$TMP in an optically transparent thin-layer electrode (OTTLE), a potential of -0.7 V[9] vs. a saturated calomel electrode (SCE) was supplied by a potentiostat that was built according to the literature.[16] For pH variation experiments, $Fe^{III}$TMP was dissolved in a 0.05 mol $dm^{-3}$ $Na_2SO_4$ solution, and concentrated $H_2SO_4$ or NaOH solutions were added with stirring, except for the highly acidic (pH <2) and basic (pH ≅12) solutions. To prepare basic solutions of pH 12-13.4, the NaOH solution of $Fe^{III}$TMP was first prepared and then $Na_2SO_4$ was added to produce

† Tohoku University.
‡ The Ohio State University.

(1) E. B. Fleischer and P. Hambright, *Inorg. Chem.*, **9**, 1757 (1970).
(2) R. F. Pasternack, H. Lee, P. Malek, and C. Spencer, *J. Inorg. Nucl. Chem.*, *39*, 1865 (1977).
(3) R. F. Pasternack and E. G. Spiro, *J. Am. Chem. Soc.*, **100**, 968 (1978).
(4) F. L. Larris and D. L. Toppen, *Inorg. Chem.*, **17**, 71 (1978).
(5) H. Goff and L. O. Morgan, *Inorg. Chem.*, **15**, 3181 (1976).
(6) D. Welnraub, P. Peretz, and M. Faraggl, *J. Phys. Chem.*, **86**, 1839, 1842 (1982).
(7) P. A. Forshey and T. Kuwana, *Inorg. Chem.*, **20**, 693 (1981).
(8) H. Kurihara, F. Arifuku, I. Ando, M. Saita, R. Nishino, and K. Ujimoto, *Bull. Chem. Soc. Jpn.*, **55**, 3515 (1982).
(9) T. Kuwana, M. Fujihira, K. Sunakawa, and T. Osa, *J. Electroanal. Chem.*, **88**, 299 (1978).
(10) T. Kuwana, R. J. Chan, and A. Battelheim, *J. Electroanal. Chem.*, **99**, 391 (1979).
(11) N. Kobayashi, M. Fujihira, K. Sunakawa, and T. Osa, *J. Electroanal. Chem.*, **101**, 269 (1979).
(12) A. Battelheim, R. J. Chem, and T. Kuwana, *J. Electroanal. Chem.*, **110**, 93 (1980).
(13) P. A. Forshey, T. Kuwana, N. Kobayashi, and T. Osa, *Adv. Chem. Ser.*, **No. 201**, 601 (1982).
(14) N. Kobayashi, T. Nozawa, and M. Hatano, *Biochim. Biophys. Acta*, **493**, 340 (1977), and ref 1-24 listed therein.
(15) B. Holmquist in "The Porphyrins", Vol. 3, D. Dolphin, Ed., Academic Press, New York and London, 1978, Part A, p 249.
(16) T. Kuwana and J. W. Strojek, *Discuss. Faraday Soc.*, **45**, 134 (1968).

0020-1669/83/1322-3608$01.50/0 

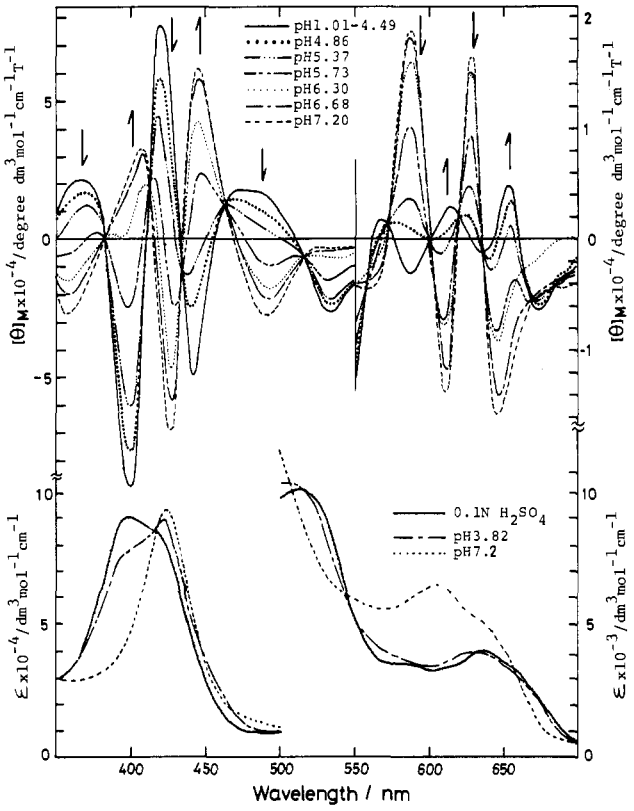


**Figure 1.** MCD (top) and absorption spectra (bottom) of $Fe^{III}TMP$ in 0.05 M $Na_2SO_4$ aqueous solutions at 20 °C. Concentrations were $1.608 \times 10^{-5}$ M (1 M = 1 mol $dm^{-3}$) for MCD and $1.76 \times 10^{-4}$ M $Fe^{III}TMP$ for absorption spectra. Cell lengths were 1 mm for the Soret and 10 mm for the visible band, respectively. Field was 1.15 T. pH was adjusted by adding concentrated $H_2SO_4$ or NaOH solution with stirring. Bold arrows indicate the direction of the MCD change with increasing pH.

a solution of 0.15 ≅ ionic strength ≅ 0.2. Also, 0.05 M $H_2SO_4$ and 1 M NaOH solutions were used. A mixture of glycerol and 0.5 mol $dm^{-3}$ phosphate buffer (pH 7.20) in the volume ratio of 2:1 was adopted as the cryogenic glassy solvent. For the measurements in the region above 1000 nm, $Fe^{III}TMP$ was dissolved in deuterated water of pD ca. 7.5 that was adjusted by concentrated DCl and NaOD solutions.

Small rectanglar OTTLEs that contained a gold minigrid as the working electrode and could fit into the cell holders of absorption and MCD apparatus were constructed according to the literature.[17,18]

**(ii) Measurement.** Absorption spectra were measured with a JASCO UVIDEC-1 spectrophotometer. MCD spectra were measured by use of JASCO J-500 and J-200 spectrodichrometers equipped with a data processor and with an electromagnet which produced magnetic fields up to 1.17 T (T = tesla), with parallel and then antiparallel fields. Its magnitude was expressed in terms of molar ellipticity per tesla (1 T = 10000 G), $[\theta]_M/10^4$ deg $mol^{-1}$ $dm^3$ $cm^{-1}$ $T^{-1}$. Cells of path lengths 1 and 10 mm were used at ambient temperature. For low-temperature measurements, a cell of 2-mm path length equipped with a Cu(Au–Co) thermocouple was placed in a quartz Dewar and the temperature was regulated by a stream of cold nitrogen gas from a container of liquid nitrogen. The path length of the OTTLE was determined to be 0.29 mm by measuring and comparing the absorbance of the Soret band of a freshly prepared $Fe^{III}TMP$ solution, whose concentration had been predetermined in a calibrated 1-cm cuvette. Values of pH were determined with a Hitachi-Horiba M-7 pH meter.

Spectra were obtained as soon as possible after the preparation of sample solutions.[8]

## Results and Discussion

**(i) Proton Equilibria. (a) Proton Equilibria between $Fe^{III}TMP$ Species.** Figures 1 and 2 show the MCD and

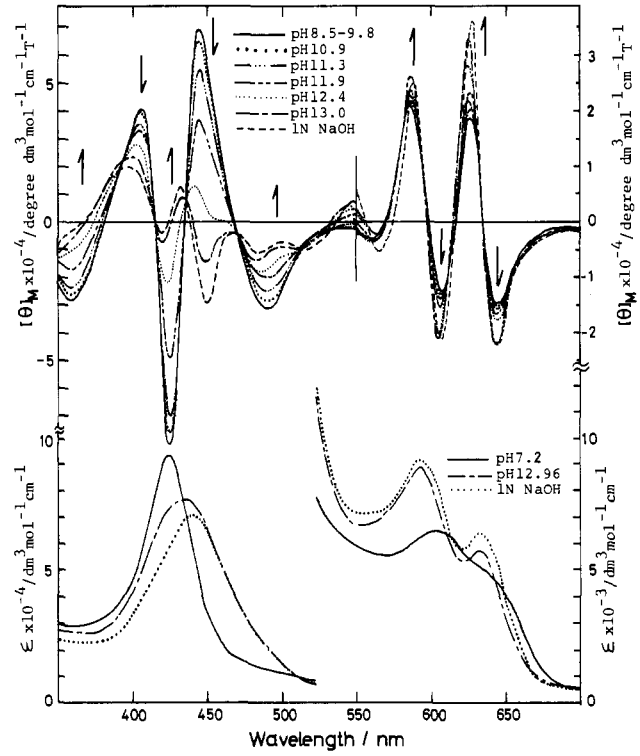


**Figure 2.** MCD (top) and absorption spectra (bottom) of $Fe^{III}TMP$ in 0.05 M $Na_2SO_4$ aqueous solution at 20 °C. Concentrations were $1.608 \times 10^{-5}$ M (pH 9.8–13.0) and $1.76 \times 10^{-4}$ M (pH 14). The spectra at pH 14 were measured in 1 M NaOH. Cell path lengths were 1 mm for the Soret and 10 mm for the visible band, respectively. Field was 1.15 T. pH was adjusted by adding concentrated NaOH solution with stirring. Bold arrows indicate the direction of MCD change with increasing pH value.

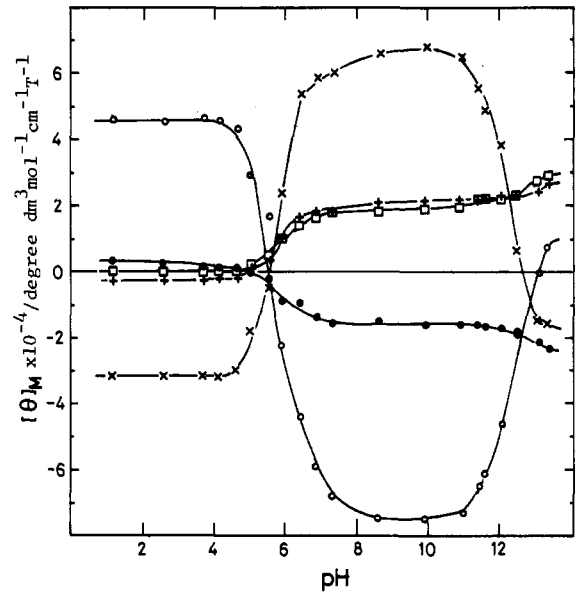


**Figure 3.** pH dependence of MCD intensity for $Fe^{III}TMP$ species at several wavelengths, replotted from Figure 1 and 2: ×, 427 nm; ○, 446 nm; □, 588 nm; +, 628 nm; ●, 645 nm.

electronic absorption spectra of $Fe^{III}TMP$ at pH values of 1.0–7.2 and 7.2–13.4, respectively. In contrast to the monotonic absorption spectra, very complex MCD spectra that exhibit high dependence on pH are observed. The dependence of the MCD intensity on pH at several wavelengths as taken from data in Figures 1 and 2 is plotted in Figure 3. As seen, three different species exist between pH 1 and 13.4 (Figure 3), and two sets of isoelliptic points appear in the transfor-

(17) T. P. DeAngelis and W. R. Heineman, *J. Chem. Educ.*, **53**, 594 (1976).
(18) C. W. Anderson, H. B. Halsall, and W. R. Heineman, *Anal. Biochem.*, **93**, 366 (1979).

Table I. Number of Transferred Protons ($n$) and Equilibrium Constant ($K_a$) Obtained from pH Titration Curves of $Fe^{III}TMP$[a]

| | M ⇌ M′ | | 2M ⇌ D | |
|---|---|---|---|---|
| λ/nm | $n$ | p$K_a$ | $n$ | p$K_a$ |
| | pH 4–8 | | | |
| 427 | 1.2 | 5.7 | 1.66 | 10.0 |
| 446 | 1.1 | 5.7 | 1.66 | 10.0 |
| 588 | 0.9 | 5.9 | 1.4 | 8.0 |
| 628 | 1.0 | 5.8 | 1.7 | 9.8 |
| 645 | 0.9 | 5.7 | 1.5 | 8.7 |
| | pH 10–14 | | | |
| 427 | 1.2 | 12.3 | 1.6 | 19.9 |
| 446 | 1.0 | 12.5 | 1.2 | 15.3 |
| 628 | 1.0 | 12.2 | | |

[a] M = monomer; M′ = monomer′; D = dimer.

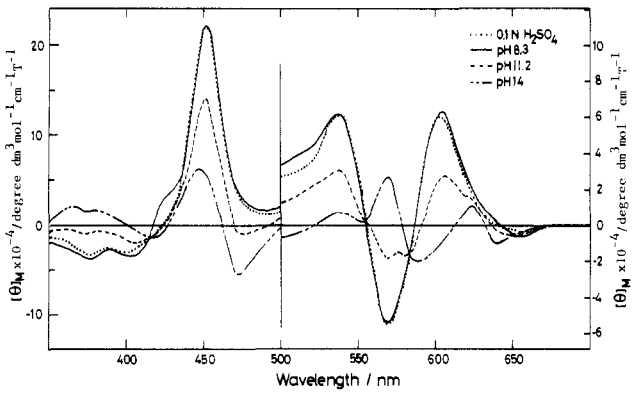


**Figure 4.** MCD spectra of $Fe^{II}TMP$ at various pH values. The samples were $1.82 \times 10^{-4}$ M in 0.05 M $H_2SO_4$ (pH 1.0), 0.1 M $NaHCO_3$ (pH 8.3), or carbonate buffer (pH 11.2) and $7.83 \times 10^{-4}$ M in 1 M NaOH (pH 14) (path length 0.29 mm (OTTLE), field 1.15 T, working electrode potential −0.7 V vs. SCE).

mation between them (Figures 1 and 2). Also, the positions of the inflection points are the same irrespective of the wavelength examined. This indicates the presence of two equilibria accompanying proton transfer: the one at pH 4–8 and the other at pH 11–14. In order to avoid the problem of monomer–dimer equilibrium, which makes the analysis difficult, we also conducted separately a Beer's law test over the concentration ranges of $5 \times 10^{-7}$–$1.8 \times 10^{-5}$ mol dm$^{-3}$ at pH 1 and 13.2, respectively, at the wavelengths of both absorption maxima (401 and 440 nm) and ellipticity maxima (403, 420, 425, and 444 nm). The clear proportionality observed between the absorbance or ellipticity and [$Fe^{III}TMP$] rule out evidence for any dimeric species in the system of the present study. Hence, from Figure 3, species at pH 1–4 and 13.2 should both be monomeric, and the former is perhaps $Fe^{III}TMP(H_2O)$, as proposed by several authors.[2,7,8] [Of course the possibility of a diaqua monomer cannot be excluded completely; however, in the relationship between the ferrous species present in the acidic solution, the possibility of a pentacoordinated species seems large (see sections i(b) and ii(b)).]

Consequently, assuming that the equilibrium between species at pH 1–4 and 8–11 can be expressed by either eq 1 or 2, we evaluated the number of transferred protons, $n$, and

$$\text{monomer} \rightarrow \text{monomer}' + n\text{H}^+ \quad (1)$$

$$2(\text{monomer}) \rightarrow \text{dimer} + n\text{H}^+ \quad (2)$$

the equilibrium constant, $K_a$, from the data in Figure 3 according to the conventional method[8,19-21] (Table I). As revealed, the equilibrium in the region of pH 4–8 obviously involves one proton transfer between different monomers, since the $n$ and p$K_a$ values estimated by eq 1 are close to 1 and to the pH value of the inflection point, respectively. Then, species between pH 8 and 11 may be presented by $Fe^{III}TMP(OH)$. Similarly, species at pH ≅13 may be specified as $Fe^{III}TMP(OH)_2$. These data accord in many respects with those obtained through the analysis of UV absorption data.[8]

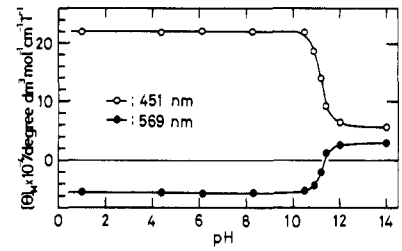


**Figure 5.** pH dependence of MCD intensity for $Fe^{II}TMP$ species at 451 and 569 nm.

Table II. Number of Transferred Protons ($n$) and Equilibrium Constant ($K_a$) Obtained from pH Titration Curves of $Fe^{II}TMP$ (pH 10–12)

| | M ⇌ M′ | |
|---|---|---|
| λ/nm | $n$ | p$K_a$ |
| 451 | 1.0 | 11.2 |
| 538 | 1.1 | 11.2 |
| 569 | 1.0 | 11.3 |

[a] M = monomer; M′ = monomer′.

**(b) Proton Equilibria between $Fe^{II}TMP$ Species.** Figure 4 shows the MCD spectra of electrochemically produced $Fe^{II}TMP$ species at pH 1 (0.05 M $H_2SO_4$), 8.3 (phosphate buffer), 11.2 (carbonate buffer), and 14 (1 N NaOH). Although the iron porphyrin concentrations in solution were larger than those of the solution used in Figures 1 and 2 by 1 order, these are the spectra of monomeric species, since electrochemical reduction of $Fe^{III}TMP$ gives only monomeric species even if the initial $Fe^{III}TMP$ solution contains dimeric $Fe^{III}TMP$ species.[7,8] In Figure 5 is shown the dependence of the MCD intensity on pH at 451 and 569 nm. The intensity does not change practically between pH 1 and 10; however, at pH above 10.5 it becomes smaller with a set of isoelliptic points and finally at pH above ca. 12.5 it reaches another constant value. Therefore, the equilibrium between species at pH 1–10 and 12.5–14 was analyzed by using eq 1 (Table II). Evidently, the number of transferred protons is 1.

**(ii) Interpretation of MCD Spectra. (a) Spectra of $Fe^{III}TMP$ Species.** The UV–visible absorption and MCD spectra of $Fe^{III}TMP$ at pH 1.0 and 7.2 as replotted from Figure 1 are shown in Figure 6. The spectra of $Fe^{III}TMP$ in DMF are also included in the figure for the purpose of comparison. The spectra in the "visible" region indicate that $Fe^{III}TMP$ is in a high-spin state both in DMF and in aqueous solution of pH 1. Although the spectra are shifted to the blue, their pattern is quite similar to that of one of the typical high-spin state complexes, (*meso*-tetraphenylporphinato)iron(III) chloride, $Fe^{III}TPP(Cl)$.[22] The Soret MCD spectrum of $Fe^{III}TMP$ at pH 1 is seemingly very complicated because of the presence of an intense trough at ca. 400 nm, which appeared for some reason presently unknown. By the change of solvent from water to DMF, however, this trough disappears to produce a "normal" type spectrum. Thus, although some

(19) E. B. Fleischer, J. M. Palmer, T. S. Srivastava, and A. Chatterjee, *J. Am. Chem. Soc.*, **93**, 3162 (1971).
(20) R. F. Pasternack and M. A. Cobb, *J. Inorg. Nucl. Chem.*, **35**, 4327 (1973).
(21) R. F. Pasternack, M. A. Cobb, and N. Sutin, *Inorg. Chem.*, **14**, 866 (1975).
(22) H. Kobayashi, M. Shimizu, and I. Fujita, *Bull. Chem. Soc. Jpn.*, **43**, 2335 (1970).

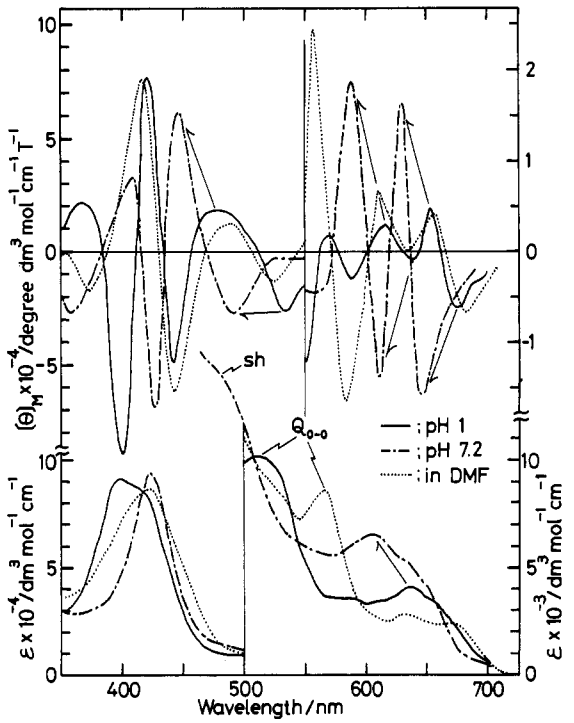


**Figure 6.** MCD (top) and absorption (bottom) spectra of $Fe^{III}TMP$ at pH 1.0 (—) and 7.2 (-·-) (0.1 M phosphate buffer) and in DMF (···). Spectra in the aqueous solution were replotted from Figure 1 ([$Fe^{III}TMP$] in DMF 4.93 × $10^{-5}$ M, path length 1 mm except in the visible region of the absorption spectra (10 mm)).

deviation from "normal" spectra is observed in the MCD spectra, $Fe^{III}TMP$ at pH 1 seems to be a high-spin state complex. This result is consistent with that obtained from the magnetic susceptibility data.[2]

The spectra of $Fe^{III}TMP$ at pH 7.2 are fairly different from those at pH 1. However, these are also likely to be those of high-spin-state complexes from the following two criteria: (1) the data in the near-IR region are suitable and satisfactory for the species to be in a high-spin state (see Figure 8) and (2) the spectral difference between the solutions of pH 1 and 7.2 can be interpreted by the explanation that Kobayashi et al. used to describe the difference among the spectra of $Fe^{III}TPP(F)$, $Fe^{III}TPP(Cl)$, and $Fe^{III}TPP(Br)$.[23] According to their data, the spectra of $Fe^{III}TPP(F)$ are shifted fairly to the blue and intensified compared with those of $Fe^{III}TPP(Cl)$ and $Fe^{III}TPP(Br)$, although they all belong to the ferric high-spin grouping. As indicated by arrows in Figure 6, the same tendency was observed among $Fe^{III}TMP$ species. Namely, the position of the visible bands shifts from $Fe^{III}TMP$ in DMF to $Fe^{III}TMP$ in water at pH 1 and further to $Fe^{III}TMP$ in water at pH 7.2. $Fe^{III}TMP$ in DMF and $Fe^{III}TMP$ in water at pH 1 reveal, associated with $Q_{0-0}$ absorption bands, sinusoidal MCD curves with a change in sign from minus to plus from the lower energy side. Hence, as is discernible in Figure 6, the 440–530 nm region MCD spectrum of $Fe^{III}TMP$ in water at pH 7.2 can be considered to be originated from its $Q_{0-0}$ absorption band. Such a phenomenon was also observed in the MCD spectra of $Fe^{III}TPP(F)$,[23] and this is the reason for the complicated Soret MCD spectrum of $Fe^{III}TMP$ at pH 7.2. Then, if we accept the result of the Kobayashi et al. calculation based on the composite molecular orbital method,[23] it appears that the (porphyrin-to-iron) charge-transfer (CT) state that interacts with the Soret state is higher in $Fe^{III}TMP$ at pH 7.2 than in that at pH 1.

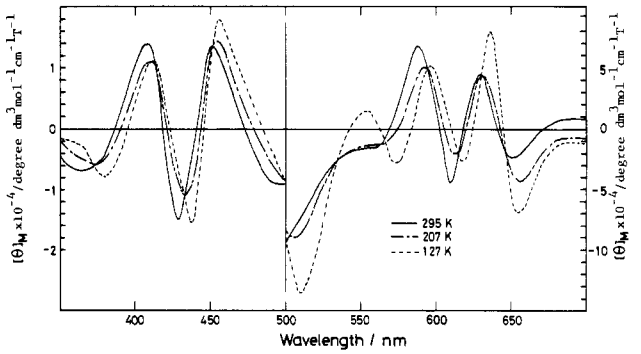


**Figure 7.** Effect of temperature on the MCD spectra of $Fe^{III}TMP$. The sample was 1.76 × $10^{-4}$ M in a solvent of 0.5 M potassium phosphate and glycerol (1:2 v/v) (pH 7.2, path length 2 mm, field 1.15 T).

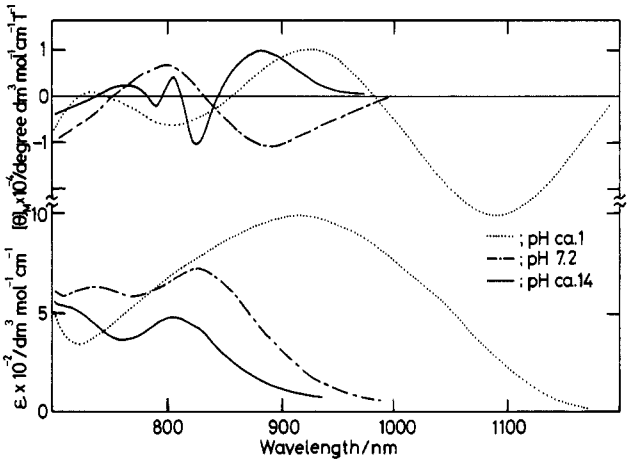


**Figure 8.** Near-IR MCD (top) and absorption (bottom) spectra of $Fe^{III}TMP$ at pH 1 (···), 7.2 (-·-), and 14 (—). [$Fe^{III}TMP$] = 1.76 × $10^{-4}$ M in 0.05 M $H_2SO_4$ or 1.76 × $10^{-5}$ M in 0.1 M phosphate buffer or 1 M NaOH. MCD spectra are the average of several scans with use of a data processor (DP-500 attachment).

The effect of temperature on the MCD of $Fe^{III}TMP$ at pH 7.2 is shown in Figure 7. Since deviations from Beer's law behavior was not observed under the experimental conditions employed, these spectra originate from monomeric species. As seen, no clear correlation between the intensity and temperature is observed through the 300–700-nm region, suggesting that the species at this pH belongs to $Fe^{III}$ high-spin porphyrins.[24,25]

Compared with the case of $Fe^{III}TMP$ at pH 1 or 7.2, few data are obtainable for $Fe^{III}TMP$ species in water at pH above 13 (Figure 2). Visible absorption spectra are more similar to those of $Fe^{III}$ low-spin porphyrins than to those of $Fe^{III}$ high-spin porphyrins, and the red-shift of the Soret band accords with the general trend of the $Fe^{III}$ high- to low-spin transition.[26-28]

The near-IR absorption and MCD spectra of $Fe^{III}TMP$ at pH ca. 1, 7.2, and 14 are shown in Figure 8. The bands of $Fe^{III}$ porphyrins in this region have been assigned to a charge-transfer (CT) band that is likely to be a porphyrin-to-iron type.[28-30] From the data accumulated, it is now

(23) H. Kobayashi, H. Kaizu, and K. Tsuji, Abstracts, 45th Annual Meeting of the Chemical Society of Japan, Tokyo, April 1982, No. 2B36.

(24) H. Kobayashi, T. Higuchi, and K. Equchi, *Bull. Chem. Soc. Jpn.*, **49**, 457 (1976).

(25) L. Vickery, T. Nozawa, and K. Sauer, *J. Am. Chem. Soc.*, **98**, 343, 351 (1976).

(26) G. Schoffa, *Adv. Chem. Phys.*, **7**, 182 (1964).

(27) T. Yonetani in "Probes of Structure and Function of Macromolecules and Membranes", Vol. 2, B. Chance, T. Yonetani, and A. S. Mildvan, Eds., Academic Press, New York and London, 1971, p 545.

(28) D. W. Smith and R. J. P. Williams, *Struct. Bonding (Berlin)*, **7**, 1 (1970).

theoretically and empirically established that typical low-spin $Fe^{III}$ porphyrins show only positive MCD spectra with shapes similar to those of absorption spectra but that representative high-spin $Fe^{III}$ porphyrins produce dispersion type MCD curves with a change in sign from minus to plus from the longer wavelength side, associated with the lowest energy absorption maxima.[14,31-37] From these points of view, the spectra manifest that both $Fe^{III}TMP$ species at pH 1 and 7.2 are classified into high-spin complexes. Besides, in accord with the results in the visible region and with the report by Smith et al.[28] that a linear relationship exists for the position of CT bands in the near-IR and visible regions, an absorption maximum of $Fe^{III}TMP$ in pH 7.2 buffer (828 nm) locates blue to that of $Fe^{III}TMP$ in 0.05 M $H_2SO_4$ (912 nm). As seen, $Fe^{III}TMP$ in pH 7.2 buffer exhibits an essentially pure Faraday *A* term associated with the strongest electronic absorption peak, implying that the effective symmetry of the iron is as close as $D_{4h}$ and, therefore, that the degeneracy in the $E_g$ excited states is not appreciably removed. In contrast, nonsymmetrical MCD spectra corresponding to the absorption peak (912 nm) are observed for $Fe^{III}TMP$ species at pH 1. Apparently the contribution of the other than an *A* term (plausibly a *C* term[37]) to the MCD spectra for $Fe^{III}TMP$ species at pH 1 is greater than that for $Fe^{III}TMP$ at pH 7.2. Hence, it is concluded that the excited-state degeneracy, i.e. the effective symmetry of the iron for $Fe^{III}TMP$ at pH 1, is lower than that for that at pH 7.2.

The MCD spectra of $Fe^{III}TMP$ at pH values above 13 are decisively different from those of the above two cases in that their pattern is plus to minus from the lower energy side. If we consider that no high-spin complexes hitherto examined showed such a pattern and that this spectral pattern is close to that of the alkaline forms of metmyoglobin[33] and peroxidase,[14] a reasonable explanation for the lowest energy positive MCD may be to ascribe it to the low-spin component.

Preliminary ESR information lends support to the above results.[8] That is, a high-spin signal with *g* value of 5.5 and a set of low-spin signals with *g* values of 1.9, 2.1, and 2.5 have been reported respectively in acidic solution and solutions with pH values above 11. The latter low-spin signals are known to grow markedly with increasing pH.

**(b) Spectra of $Fe^{II}TMP$ Species.** Heretofore, $Fe^{II}TMP$ species have been less well characterized compared with $Fe^{III}TMP$ species.[7] The MCD spectra of $Fe^{II}TMP$ are practically independent of pH between pH values 1 and 10 (Figures 4 and 5) and can be classified into the $Fe^{II}$ high-spin grouping from the characteristic shape of the Soret band.[25,38,39] In an optical spectrum, the corresponding peaks appear at 445 ($\epsilon$ 148 000) and 562 nm.[7] Since four-coordinate square-planar iron(II) tetraarylporphyrins are known to have two bands of roughly equal intensity of opposite signs in the Soret region (350–500 nm),[40] the species would have at least one axial ligand. Although it is not easy to distinguish between five- and six-coordination, the magnitude and the shape of the bands are more similar to those of five-coordinated species.[41] On the other hand, the spectra above pH 12.5 are exemplary for diamagnetic low-spin species.[25,39,42,43] As is expected from MCD theory,[42,43] substantially pure Faraday *A* terms are detected associated with three absorption maxima at 456 ($\epsilon$ $9.9 \times 10^{-4}$), 575 ($\epsilon$ $11.3 \times 10^{-3}$), and 619 nm ($\epsilon$ $6.4 \times 10^{-3}$).[7] The possibility of a $\mu$-oxo dimer may be small from comparison of the spectrum with that of a reference compound, $[Fe^{II}TPP]_2O$, which produces a broad S-shaped curve distinguishable from the sharper bands of the normal porphyrin complexes.[41]

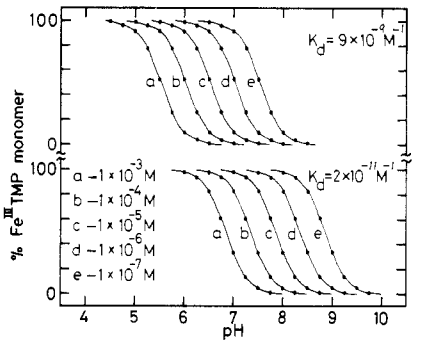


**Figure 9.** Percent of $Fe^{III}TMP$ monomer as a function of pH for (a) $1 \times 10^{-3}$ M, (b) $1 \times 10^{-4}$ M, (c) $1 \times 10^{-5}$ M, (d) $1 \times 10^{-6}$ M, and (e) $1 \times 10^{-7}$ M total iron porphyrin concentration. The upper curves were calculated by utilizing the $K_d$ value of $9 \times 10^{-9}$ $M^{-1}$, and the lower curves, the value of $2 \times 10^{-11}$ $M^{-1}$.

**(iii) The Monomer–Dimer Equilibria.** A monomer–dimer equilibrium for $Fe^{III}TMP$ has been reported by several authors. The dimerization constant, $K_d$, for eq 3 has been determined

$$2Fe^{III}TMP \xrightarrow{K_d} (Fe^{III}TMP)_2O + 2H^+ \qquad (3)$$

to be $9 \times 10^{-4}$ $M^{-1}$, $2 \times 10^{-11}$, $3 \times 10^{-9}$ $M^{-1}$, and $7 \times 10^{-10}$ $M^{-1}$ by Pasternack et al.,[2,3] Forshey et al.,[7] Goff et al.,[5] and Welnraub et al.,[6] respectively.[44] Using the largest and the smallest $K_d$ values, we calculated the percent of $Fe^{III}TMP$ monomer as a function of pH for (a) $1 \times 10^{-3}$ M, (b) $1 \times 10^{-4}$ M, (c) $1 \times 10^{-5}$ M, (d) $1 \times 10^{-6}$ M, and (e) $1 \times 10^{-7}$ M total iron porphyrin concentrations (Figure 9). Evidently, the percentage of $Fe^{III}TMP$ monomer at fixed pH values increases with the decrease of [total iron porphyrin], and the diluter the solution and the smaller the $K_d$ value, the more the inflection points of the monomer–dimer transition shift to alkaline pH. As judged, however, there is a discrepancy between these data and ours or Kurihara's.[8] That is, according to these graphs, the percentage of $Fe^{III}TMP$ monomer at pH 9 for the solution of [total iron porphyrin] of $1 \times 10^{-5}$ M (curve c) is negligibly small. Nevertheless indication of dimer formation was not observed in our and Kurihara's experiments conducted at nearly the same [total iron porphyrin] range (Figures 1 and 2 and the results of Beer's law tests). Depending on the interpretation of this fact, several possibilities are conceivable.

(29) P. Day, D. W. Smith, and R. J. P. Williams, *Biochemistry*, **6**, 1563, 3747 (1967).
(30) M. Zerner, M. Gouterman, and H. Kobayashi, *Theor. Chim. Acta*, **6**, 363 (1966).
(31) J. C. Cheng, G. A. Osborne, P. J. Stephens, and W. A. Eaton, *Nature (London)*, **241**, 193 (1973).
(32) P. J. Stephens, J. C. Sutherland, J. C. Cheng, and W. A. Eaton in "Proceedings of the International Conference on Excited States of Biological Molecules, Leiden", J. Birks, Ed., Wiley-Interscience, New York, 1976, p 434.
(33) T. Nozawa, T. Yamamoto, and M. Hatano, *Biochim. Biophys. Acta*, **427**, 28 (1976).
(34) J. Rawlings, P. J. Stephens, L. A. Nafie, and M. D. Kamen, *Biochemistry*, **16**, 1725 (1977).
(35) T. Nozawa, T. Shimizu, M. Hatano, H. Shimada, T. Iizuka, and Y. Ishimura, *Biochim. Biophys. Acta*, **534**, 285 (1978).
(36) N. Kobayashi, T. Nozawa, and M. Hatano, *Bull. Chem. Soc. Jpn.*, **54**, 919 (1981).
(37) T. Yamamoto, T. Nozawa, N. Kobayashi, and M. Hatano, *Bull. Chem. Soc. Jpn.*, **55**, 3059 (1982).
(38) N. Kobayashi, T. Nozawa, and M. Hatano, *Biochem. Biophys. Acta*, **427**, 652 (1976).
(39) M. Hatano and T. Nozawa, *Adv. Biophys.*, **11**, 95 (1978).
(40) J. P. Collman, J. I. Brauman, K. M. Doxsee, T. R. Halbert, E. Bunnenberg, R. E. Rinder, B. N. LaMar, J. D. Gaudio, G. Lang, and K. Spartalian, *J. Am. Chem. Soc.*, **102**, 4182 (1980).
(41) J. P. Collman, F. Basolo, E. Bunnenberg, T. J. Collins, J. H. Dawson, P. E. Ellis, Jr., M. L. Marrocco, A. Moscowitz, J. L. Sessler, and T. Szymanski, *J. Am. Chem. Soc.*, **103**, 5636 (1981).
(42) J. C. Sutherland and M. P. Klein, *J. Chem. Phys.*, **57**, 76 (1972).
(43) P. J. Stephens, W. Suetaka, and P. N. Schatz, *J. Chem. Phys.*, **44**, 4592 (1966).
(44) Because of the difference in definition, $K_d$ values by Pasternack[2,3] and Forshey[7] were divided by the ionic product of water, $K_w = 1 \times 10^{14}$, and compared with $K_d$ obtained by Welnraub.[6]

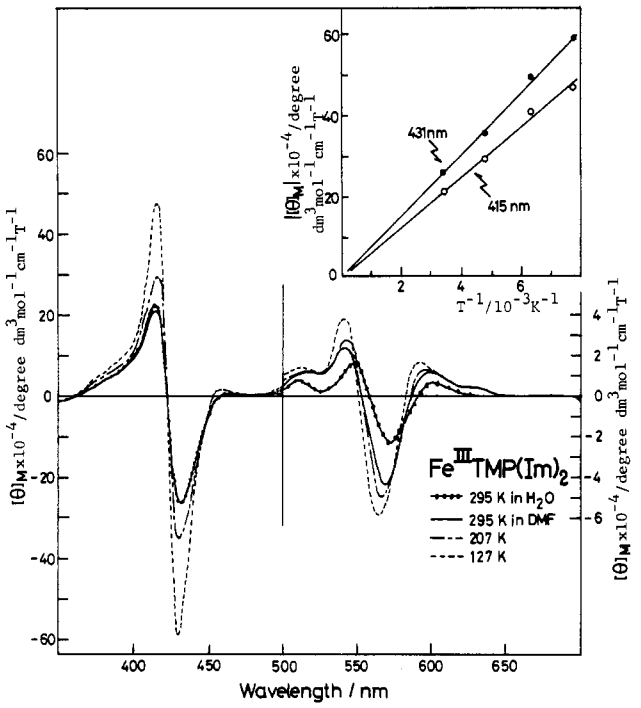


**Figure 10.** MCD spectra of $Fe^{III}TMP(Im)_2$ in water at pH 7.2 at 295 K (-•-•) and in DMF at 295 (—), 207 (-·-), and 127 K (···). [$Fe^{III}TMP$] in water = $1.76 \times 10^{-4}$ M with [Im] = 0.5 M in a 2:1 v/v mixture of glycerol–0.5 M phosphate buffer, pH 7.2. The inset shows a plot of the MCD intensity at 431 (●) and 415 nm (○) vs. the reciprocal of the absolute temperature (path length for low-temperature measurements 2 mm, field 1.15 T).

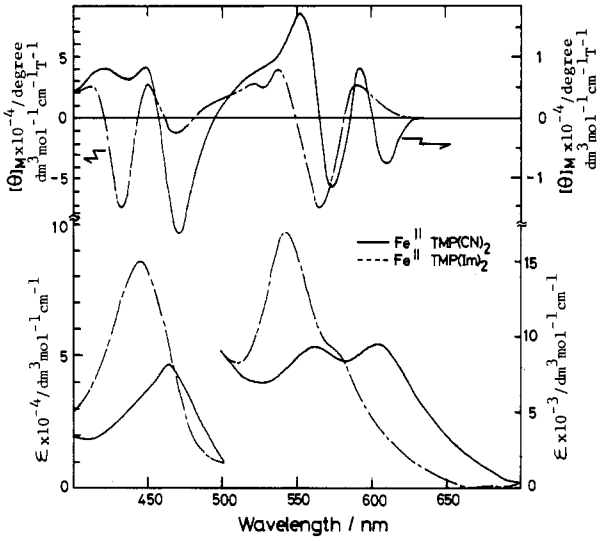


**Figure 11.** MCD (top) and absorption spectra (bottom) of $Fe^{II}TMP(Im)_2$ (-·-) and $Fe^{II}TMP(CN)_2$ (—). [$Fe^{II}TMP$] = $1.76 \times 10^{-4}$ M, [KCN] = 0.1 M, [Im] = 0.5 M, and [$Na_2S_2O_4$] = 2.2 M in 0.2 M phosphate buffer, pH 7.20 (field 1.1 T, path length 10 mm except the Soret region of the absorption spectra (1 mm)).

First, if all the data are correct, it appears that the spectra of monomeric and dimeric species are fortuitously the same so that they cannot be distinguished from each other. This possibility is however denied by the finding that p$K_a$ values of $Fe^{III}TMP$ species at pH 1–4, pH 7–10, and pH above 13 do not agree with experimentally obtained ones unless monomer–monomer transition, eq 1, is taken into account (Table I). Second, if we suppose that our and Kurihara's data alone are correct, then $K_d$ must be smaller by several orders in the context that any dimeric species could not be detected spectrophotometrically in the pH range of 1–13 for the solution containing (1–2) $\times 10^{-5}$ M total iron porphyrin. Third, if Forshey's electrochemical data alone are assumed to be correct, we cannot but consider an electrochemically detectable by spectrophotometrically inert dimer.[45] Although, a definite conclusion cannot be given, of course, at the present stage, the above discrepancy may happen to simply depend only on the difference in ionic strengths of the solutions employed.

**(iv) Spectra in the Presence of Extraneous Ligands.** By the addition of imidazole (Im) or KCN to the solution containing $Fe^{III}TMP$ or $Fe^{II}TMP$, their bisadducts ($Fe^{III}TMP(Im)_2$ $Fe^{III}TMP(CN)_2$, $Fe^{II}TMP(Im)_2$, and $Fe^{II}TMP(CN)_2$), which have been considered to be low-spin complexes, are formed.[3,6] The characteristics of MCD spectra of these species are briefly described here.

As shown in Figure 10, the UV–visible spectra of $Fe^{III}TMP(Im)_2$ in water or in DMF are typical for $Fe^{III}$ low-spin complexes.[24,25] Temperature variation experiments (inset) reveal the contribution of only Faraday $C$ terms to the Soret MCD spectra. Although not shown, the spectrum of $Fe^{III}TMP(CN)_2$ in this region is also reasonable as one of $Fe^{III}$ low-spin complexes, revealing derivative-shaped curves corresponding to the absorption maxima (the spectrum is red-shifted by 12–16 nm compared to that of $Fe^{III}TMP(Im)_2$ and its magnitude in the Soret band is ca. 78% of that of $Fe^{III}TMP(Im)_2$). The near-IR spectra of these complexes are also exemplary for $Fe^{III}$ low-spin derivatives.[14,31-37] The shape of MCD spectra are close to those of absorption spectra[46] and their sign is plus throughout the region.

Scheme I

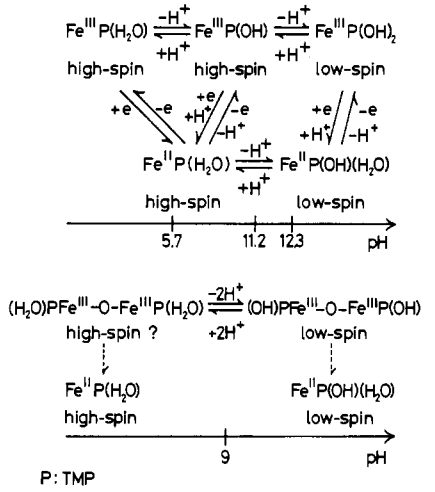


In Figure 11 are exhibited the spectra for $Fe^{II}TMP(Im)_2$ and $Fe^{II}TMP(CN)_2$ in the UV–visible region. Judging from theory,[42,43] the MCD spectra of $Fe^{II}$ low-spin porphyrins should in general be the most easily intelligible among those of the iron porphyrins. In fact, in agreement with the prediction from the theory,[42,43] most of the $Fe^{II}$ low-spin complexes reported so far showed temperature-independent Faraday $A$ terms at the position of absorption peaks.[25,39] The spectra in Figure 11 are, however, somewhat different from this respect: the MCD spectra in the Soret region are not so simple and their intensities are considerably weaker than those of hitherto examined $Fe^{II}$ low-spin complexes. The detailed description

(45) In connection with this, the presence of $Fe^{III}TMP$ forms that are inert to both the spectrophotometric and electrochemical detection was suggested in highly basic solution.[8]

(46) In $D_2O$ of pD ca. 7.5, $Fe^{III}TMP(CN)_2$ has three absorption peaks at 1666, 1473, and 1273 nm with absorption coefficients ($\epsilon$) of 420, 284, and 213 dm$^3$ mol$^{-1}$ cm$^{-1}$, respectively, while $Fe^{III}TMP(Im)_2$ has two peaks at 1330 and 1163 nm and a shoulder at 1016 nm with $\epsilon$ of 264, 292, and 206 dm$^3$ mol$^{-1}$ cm$^{-1}$, respectively.

of the spectra of various $Fe^{II}TMP$ low-spin derivatives will be published elsewhere.[47]

## Concluding Remarks

The major monomeric species in water and their spin states as deduced from the present study and in consideration of previously reported works are shown in Scheme I. Three ferric and two ferrous species are sufficient to explain the results between pH 1 and 14. Proton equilibria exist between the three ferriporphyrin species with $pK_a$ values of ca. 5.7 and 12.3. A proton equilibrium also exists between the ferroporphyrin species with a $pK_a$ value ca. 11.2. Although both $Fe^{III}TMP$ species in regions of pH 1–4 ($Fe^{III}TMP(H_2O)$) and pH 8–11 ($Fe^{III}TMP(OH)$) belong to $Fe^{III}$ high-spin complexes, the difference is that the CT state for the latter is higher than that for the former both in the visible (transition from $b_{2u}(\pi)$ and $a_{2u}(\pi)$ to $e_g(d\pi)$ in a $D_{4h}$ notation) and in the near-IR ($a_{1u}(\pi)$ and $a_{2u}(\pi)$ to $e_g(d\pi)$) regions.[28-30,33,37] Although, little information was obtained on $Fe^{III}TMP$ dimers in the present study, their relation obtained from the electrochemical experiments[7,8] is included in the lower half of Scheme I. It is noteworthy that the spin state of $Fe^{III}TMP$ in solution phase is different from that in solid phase in the pH region of 6.5–11. Namely, solid samples obtained from solutions of pH 6.5–11 are low spin.[3,5]

The MCD behaviors of $Fe^{III}TMP(Im)_2$ and $Fe^{III}TMP(CN)_2$ are representative of $Fe^{III}$ low-spin porphyrins throughout the UV to near-IR regions, while those of $Fe^{II}TMP(Im)_2$ and $Fe^{II}TMP(CN)_2$ are somewhat atypical for $Fe^{II}$ low-spin complexes in that the Soret-band spectra are complicated and weak.

**Acknowledgment.** We thank Professor M. Hatano for use of the MCD apparatus. This research was partially supported by Grant-in-Aid for Scientific Research No. 57470105 from the Ministry of Education, Science and Culture in Japan.

**Registry No.** $Fe^{III}TMP$, 60489-13-6; $Fe^{II}TMP$, 71794-64-4; $Fe^{III}TMP(Im)_2$, 72595-74-5; $Fe^{II}TMP(Im)_2$, 87306-61-4; $Fe^{II}TMP(CN)_2$, 87306-62-5.

(47) N. Kobayashi and T. Osa, manuscripts in preparation.

Contribution from the Inorganic Chemistry Laboratory, University of Oxford, Oxford, U.K., and School of Chemical Sciences, University of East Anglia, Norwich NR4 7TJ, U.K.

# Electronic Structure of Molybdenocene and Tungstenocene: Detection of Paramagnetism by Magnetic Circular Dichroism in Argon Matrices

P. ANTHONY COX,[1a] PETER GREBENIK,[1a] ROBIN N. PERUTZ,*[1a] MARK D. ROBINSON,[1a] ROGER GRINTER,[1b] and DAVID R. STERN[1b]

*Received February 15, 1982*

The magnetic circular dichroism (MCD) spectra are reported for $WCp_2$ and $MoCp_2$ (Cp = $\eta$-$C_5H_5$) generated in argon matrices by photolysis of $MCp_2H_2$. The spectra show a strong temperature dependence of intensity (*C* term), proving that these metallocenes are paramagnetic in their ground state. The photolysis of $W(MeCp)_2(C_2H_4)$ (MeCp = $\eta$-$C_5H_4CH_3$) in Ar matrices is reported to yield $W(MeCp)_2$. IR and UV data for $W(MeCp)_2$ are used to assist in assignments of absorptions of $WCp_2$. A method of analysis is developed in which spin–orbit coupling is treated as the dominant perturbation of the ground $^3E_{2g}$ state of the metallocenes. This method is applied to assign the infrared electronic absorptions of $WCp_2$ and $W(MeCp)_2$ to transitions between spin–orbit substates ($E_{1g} \leftarrow E_{2g}$). The spin–orbit coupling is shown to quench the dynamic Jahn–Teller effect in the ground state of $WCp_2$, but the off-diagonal Jahn–Teller term is much more significant for $MoCp_2$. The same method, used for the analysis of the MCD spectrum, shows that the sign and magnitude of $\Delta A/A$ (the ratio of the integrated differential absorption to the integrated absorption) for the lowest energy UV bands of both complexes are consistent with an $E_{2u} \leftarrow E_{2g}$ transition. This method sets a lower limit to $g_\parallel$ of 3.4 ± 0.7 ($WCp_2$) and 2.0 ± 0.2 ($MoCp_2$). Comparisons of the UV spectra of several metallocenes provide evidence that these are ligand-to-metal charge-transfer bands. It is shown that spin–orbit coupling lifts the symmetry restrictions on the reactivity of the $d^4$ metallocenes. The example of the paramagnetism of $WCp_2$ leads to the suggestion that paramagnetic intermediates may be important in many C–H insertion reactions.

## Introduction

The metallocenes of molybdenum and tungsten have been postulated as intermediates in a number of reactions, most notably the C–H activation reactions of $WCp_2H_2$ and $WCp_2(CH_3)H$ (Cp = $\eta$-$C_5H_5$).[2] Recently, we described the characterization of these unstable metallocenes by matrix-isolation methods and have shown that they adopt a parallel sandwich structure.[3] Molybdenocene and tungstenocene were generated by photoelimination from $MCp_2(X)Y$ (X = Y = H, M = Mo, W; X = H, Y = $CH_3$, M = W) and $MCp_2L$ (L = CO, M = Mo, W; L = $C_2H_4$, M = W) complexes and were characterized by IR and UV/vis spectroscopy. Notably, the IR spectrum of $MoCp_2$ resembled that of $CrCp_2$ in showing broad IR bands between 750 and 800 $cm^{-1}$ and only one low-frequency skeletal mode. In accord with this, we postulated that $MoCp_2$ has an electronic ground state similar to that of $CrCp_2$, viz. a $^3E_{2g}$ state subject to both Jahn–Teller and spin–orbit effects. In contrast, $WCp_2$ showed a sharp IR spectrum with two low-frequency skeletal modes and an unusual electronic IR band at 3240 $cm^{-1}$. This difference was rationalized by the larger spin–orbit coupling constant of tungsten, which reduces the degeneracy of the ground state to a spin–orbit doublet ($E_{2g}$). The electronic IR band was assigned to an intraconfigurational vibronically allowed $E_{1g} \leftarrow E_{2g}$ transition.[3] (This corresponds to an $\Omega = 1 \leftarrow \Omega = 3$ transition in the closely related $C_{\infty v}$ point group, where $\Omega$ is

* To whom correspondence should be addressed at the Department of Chemistry, University of York, York Y01 5DD, U.K. No reprints available.

(1) (a) University of Oxford. (b) University of East Anglia.
(2) Berry, M.; Cooper, N. J.; Green, M. L. H.; Simpson, S. J. *J. Chem. Soc., Dalton Trans.* **1980**, 29. Berry, M.; Elmitt, K.; Green, M. L. H. *Ibid.* **1979**, 1950. Cooper, N. J.; Green, M. L. H.; Mahtab, R. *Ibid.* **1979**, 1557. Thomas, J. L.; Brintzinger, H. H. *J. Am. Chem. Soc.* **1972**, *94*, 1386. Thomas, J. L. *Ibid.* **1973**, *95*, 1838.
(3) Chetwynd-Talbot, J.; Grebenik, P.; Perutz, R. N. *Inorg. Chem.* **1982**, *21*, 3647.

0020-1669/83/1322-3614$01.50/0 